B.TECH. PROJECT REPORT PREPARATION

INSTITUTE OF ENGINEERING & MANAGEMENT
Good Education, Good Jobs

INSTITUTE OF ENGINEERING & MANAGEMENT

SALT LAKE,

KOLKATA 700091

Fabrication-Aware Design and Dynamic Modeling of a Lightweight Fixed-Wing VTOL UAV with Autonomous Attitude Control via AHRS

SUBMITTED BY

1. **Akash Pandey**
2. **Sumit Paul**
3. **Avinash Mishra**

Report submitted for the partial fulfillment of

the requirements for the degree

of

BACHELOR OF TECHNOLOGY

Department of Mechanical Engineering

DEPARTMENT OF MECHANICAL ENGINEERING

INSTITUTE OF ENGINEERING & MANAGEMENT

MAULANA ABUL KALAM AZAD UNIVERSITY OF TECHNOLOGY,

WEST BENGAL

2025

Fabrication-Aware Design and Dynamic Modeling of a Lightweight Fixed-Wing VTOL UAV with Autonomous Attitude Control via AHRS

Akash Pandey (11)

Sumit Paul (09)

Avinash Mishra (16)

……………………………...

Supervisor 1

Prof. Barun Das

……………………………….

Supervisor 2

Prof. Joydip Ray

DEPARTMENT OF MECHANICAL ENGINEERING

INSTITUTE OF ENGINEERING & MANAGEMENT, KOLKATA

DEPARTMENT OF MECHANICAL ENGINEERING

CERTIFICATE

This is to certify that the Project/Thesis Report on "**Fabrication-Aware Design and Dynamic Modeling of a Lightweight Fixed-Wing VTOL UAV with Autonomous Attitude Control via AHRS**" is submitted in partial fulfillment of the requirements for the degree of Bachelor of Mechanical Engineering by the following students:

Akash Pandey	**(Roll No.11)**
Sumit Paul	**(Roll No.09)**
Avinash Mishra	**(Roll No.16)**

Supervisor1
Prof. Barun Das

Supervisor2
Prof. Joydip Ray

Head of the Department

Principal

Project Report Approval for B.Tech.

This project report entitled "**Fabrication-Aware Design and Dynamic Modeling of a Lightweight Fixed-Wing VTOL UAV with Autonomous Attitude Control via AHRS**" by Akash Pandey, Sumit Paul, Avinash Mishra is approved for the degree of Bachelors of Technology in Mechanical Engineering.

Examiner(s)

1………………………………

2……………………………….

Date:

Place:

ACKNOWLEDGEMENT

I would like to express my sincere gratitude to **Prof. Barun Das** and **Prof. Joydip Ray** for their invaluable guidance, support, and encouragement throughout the course of this project. Their expertise and insights have been instrumental in shaping the direction and depth of this research.

I am also deeply thankful to my fellow classmates for their constant support, collaboration, and constructive feedback, which have greatly enhanced the quality and progress of this work.

Finally, I extend my gratitude to all those who have directly or indirectly contributed to the successful completion of this project. Your assistance and encouragement have been truly invaluable.

……………………..........

(Signatures)

…………………………………..

(Name and Roll no of the student(s))

Date:

DECLARATION OF ORIGINALITY AND COMPLIANCE OF ACADEMIC ETHICS

I hereby declare that this thesis **Fabrication-Aware Design and Dynamic Modeling of a Lightweight Fixed-Wing VTOL UAV with Autonomous Attitude Control via AHRS** contains a literature survey and original project/research work carried out by me, the undersigned candidate, as part of my studies in the Department of Mechanical Engineering.

All information in this document has been obtained and presented in accordance with academic rules and ethical conduct. I also declare that, as required by these rules and regulations, I have fully cited and referenced all material and results that are not original to this work.

Details:

- Name: Akash Pandey, Sumit Paul, Avinash Mishra
- Examination Roll No: 12022002007016, 12022002007015, 22023002007005

I affirm that the work presented is original and all sources have been duly acknowledged.

Signature:

TABLE OF CONTENTS

ABSTRACT

This study presents the aerodynamic design process of a Fixed-Wing Vertical Take-Off and Landing (VTOL) Unmanned Aerial Vehicle (UAV), focusing on both the conceptual and preliminary design phases. In the conceptual design phase, multiple configurations were explored by different design teams following a common framework and mission requirements. After an evaluation and refinement process, a single optimized design concept was established as the foundation for the preliminary design phase. The preliminary design phase focused on key aerodynamic components, including fuselage shaping, wing design, stability and control analysis, empennage configuration, and winglet optimization. Additionally, the sizing of inlets and cooling systems was carefully addressed. Analytical methods and computational fluid dynamics (CFD) simulations were employed at each stage to validate and refine the design. A novel manufacturing approach using Fused Deposition Modeling (FDM) was integrated into the design process to improve structural integrity, cost-effectiveness, and production efficiency. The final UAV concept, including its geometric, aerodynamic, stability, and performance characteristics, is presented and discussed in detail.

Keywords: Fixed-Wing VTOL, UAV, Aerodynamic Design, Fuselage Shaping, Wing Optimization, Stability and Control, Computational Fluid Dynamics (CFD), Fused Deposition Modeling (FDM), Structural Integrity, Performance Analysis.

Chapter-1

INTRODUCTION

1.1 Background and Motivation

Recently, there has been a drastic paradigm shift of use of unmanned aerial vehicles (UAVs) from military operations to civilian and urban applications. In this context, one of the popular UAV applications is package delivery. When it comes to a delivery operation, accessibility of delivery location is a decisive factor. Figure 1.1a depicts a sample delivery vehicle where the main arrival point is on Pulau Ubin, Singapore. Delivering daily items from Singapore to such areas with ground vehicles would be problematic, whereas aerial delivery may be attractive. However, endurance of the aerial vehicle plays a critical role as it determines the range of the UAV. Therefore, conventional multirotors may not have sufficient flight endurance for long range applications and thus inspirational designs with wings such as in Fig. 1.1b will help to deliver items to wider ranges including the routes above seaways. It can be seen that the novel systems are not similar to classical multirotors or fixed–wing vehicles.

In addition to civilian applications, military missions, e.g. surveillance, may require the vehicle to remain airborne for longer duration. Besides, the ability to take–off and land vertically to a limited area such as on a ship would be of great advantage (see

(a) A parcel delivery route by Singpost [1]. (b) DHL Delivery Drone [2].

Figure 1.1: UAV delivery applications.

Fig. 1.2). Therefore, VTOL UAVs may be a solution to the problem of endurance and lack of runway in military missions. From this perspective, achieving a successful transition flight without stalling between the two steady conditions is a requirement for these systems. Hence, this research is motivated by the need for understanding the transition flight dynamics as well as its control, especially under varying flight conditions.

Maintenance or replacement of damaged components of a UAV poses a challenge for operational success. Most UAV users do not have access to large machine shops or specialized equipment at the mission area. To this end, a study for the suitability of use of additive manufacturing (AM) is conducted. Since on-demand manufacturing is an option with AM, maintenance or repair work can be carried out when necessary, which allows for less amount of stock parts, especially for off-shore UAV applications. In this context, various means of manufacturing are examined for different parts to assess the weight-to-strength reductions.

1.2 Challenges

1. **Operational Maintenance and Manufacturability**

   As UAV systems become more advanced and multifunctional, their structural complexity increases, leading to higher production costs. Traditional manufacturing techniques, such as injection molding for plastics or machining and drilling for metals, often result in significant material waste and are labor-intensive due to the need for multiple processing stages. These methods also restrict design innovation, limiting engineers to conventional approaches and making it challenging to realize complex, multifunctional UAV architectures.

   To overcome these constraints, composite materials like carbon fiber have gained popularity due to their excellent strength-to-weight ratio, particularly in multirotor UAV applications. However, the use of carbon fiber involves high material costs, complex fabrication steps, and limits the ability to create intricate internal geometries—especially in components such as wings.

   Additive Manufacturing (AM) presents a viable alternative by enabling free-form fabrication. As a layer-by-layer process, AM allows for the production of complex internal and external geometries that are difficult or impossible to achieve with conventional methods. It eliminates the need for casting, molding, or additional tooling for fine details. Design changes can be made directly within the CAD model without altering the production setup, enabling rapid prototyping and customization. This flexibility, combined with reduced labor requirements and faster production cycles, makes AM a promising solution for producing lightweight, multifunctional UAV structures efficiently and cost-effectively.

2. **Aerodynamic Modeling of Transition Flight**

   The flight profile of a hybrid UAV includes several distinct stages: vertical take-off, hovering, transition to forward flight, reverse transition back to hover, and landing. Accurately modeling this sequence is a key challenge. In particular, convertiplane-type UAVs operate under conditions that extend beyond low-angle, linear aerodynamic assumptions to include the nonlinear effects that arise in the flow region behind the propeller.

   The transition phases are especially critical, as they involve rapid changes in aerodynamic forces and moments. These abrupt shifts must be understood and modeled using both unsteady and quasi-steady aerodynamic frameworks to ensure accurate predictions of flight behavior and system performance.

3. **Control During Transition Phases**

   Transitioning between hover and forward flight modes is not only a modeling issue but also a complex control problem. Often, simplified approaches are used, where flight controllers are independently optimized for hover and forward flight without addressing the transition phase in detail. However, the transition path and overall flight behavior are strongly influenced by how the vehicle manages altitude, the speed of transition, and the available control inputs.

   As such, developing robust control strategies for managing the transition under varying conditions—including wind disturbances or rotor failure—is an important area of research. The effectiveness of traditional PID controllers compared to more advanced control algorithms also merits thorough investigation, particularly for ensuring stability and performance throughout the full flight envelope of hybrid UAVs.

Chapter-2

LITERATURE REVIEW

2.1 UAS Design Configurations

[1]Unmanned Aerial Vehicles (UAVs) come in various configurations, each tailored to meet specific operational needs such as endurance, maneuverability, payload capacity, and takeoff/landing constraints. The most common configurations include multirotors, fixed-wing, and hybrid VTOL (Vertical Take-Off and Landing) systems. Multirotor UAVs offer high stability and vertical lift capabilities, making them ideal for hovering and short-range missions, but they are limited by low aerodynamic efficiency and reduced flight endurance. Fixed-wing UAVs, on the other hand, provide superior lift-to-drag ratios, enabling longer flight times and higher speeds; however, they require runways or launch mechanisms for operation. Hybrid configurations such as tilt-rotor, tilt-wing, and tail-sitter designs aim to combine the benefits of both systems by enabling vertical takeoff and efficient forward flight. These designs are particularly relevant for operations where runway availability is limited but extended range is necessary. The choice of configuration depends heavily on mission objectives, environmental conditions, and logistical constraints.

2.2 Additive Manufacturing (AM)

Additive Manufacturing (AM) initially emerged as a rapid prototyping technique, enabling engineers to detect and rectify dimensional discrepancies, structural inadequacies, and conceptual design flaws during early development phases. Through its capacity for expedited fabrication and reduced tooling requirements, AM has become an indispensable tool in the iterative design and validation process. With advances in material science and machine capabilities, its scope has expanded from prototyping to direct fabrication of end-use components, particularly for complex and low-volume aerospace applications.

The inherent advantages of AM include reduced lead time, lower production costs for intricate geometries, and minimal material wastage due to its layer-by-layer fabrication strategy. These benefits are especially valuable in the production of lightweight UAV components, where structural efficiency and mass reduction are critical. Unlike traditional subtractive and formative manufacturing methods, AM eliminates the need for extensive tooling, multi-step fabrication, and excess raw material consumption—challenges that often limit the feasibility of producing geometrically complex structures.

A core requirement for AM is an accurate solid CAD model, which simplifies the design-to-manufacturing pipeline. However, the fidelity of the final part is highly sensitive to design accuracy, particularly for structures with high geometric complexity. Design revisions, though, can be seamlessly integrated into the CAD model without necessitating changes to the manufacturing setup, thereby offering substantial flexibility in iterative development. A notable limitation remains the restricted build envelope of AM systems, necessitating the segmentation of large UAV components into multiple assemblies. Additionally, post-processing steps—such as surface finishing—are often essential to enhance aerodynamic efficiency, especially for components like wings where surface roughness can significantly influence lift-to-drag performance.

Advanced design methodologies have been adopted to maximize the structural potential of AM. [2]Lattice structures, including periodic honeycombs, foams, and truss-based configurations, are increasingly employed due to their high stiffness-to-weight ratios and energy absorption capabilities. Topology optimization techniques are used to computationally determine optimal material distribution within a design domain, facilitating maximum load-bearing efficiency with minimal mass. While computationally intensive, this approach is particularly advantageous in critical UAV substructures such as spars and brackets. Bio-inspired geometries, modeled after load-efficient structures found in nature, offer another strategy for minimizing material use while preserving mechanical integrity, particularly under aerodynamic loading.

Infill optimization—a method unique to AM—allows designers to tailor internal geometries by manipulating infill density, pattern, and orientation. While effective in reducing overall part weight and material usage, this approach can lead to uniform reductions in mechanical strength if not selectively applied, necessitating careful evaluation based on functional loading conditions.

In conclusion, Additive Manufacturing presents a compelling alternative to conventional fabrication techniques for UAV structures, offering unprecedented design freedom, material efficiency, and rapid iteration capabilities. However, challenges related to build volume constraints, post-processing requirements, and surface integrity must be addressed to fully exploit its potential in high-performance aerospace applications.

2.3 Additive Manufacturing and Lightweight Structural Design

Lattice Structures and Topology Optimization.......

Sandwich structures with periodic cellular cores—such as lattices, honeycombs, and trusses—are widely utilized in aerospace and automotive industries due to their high strength-to-weight and stiffness-to-weight ratios. Among these, truss and honeycomb geometries are preferred for their efficient energy absorption and in-plane stiffness.

Topology optimization is a computational method used to determine the optimal material layout within a given design space, maximizing stiffness while minimizing weight. This is particularly valuable for UAV components like wings or brackets, despite its high computational cost. Bio-inspired designs, derived from natural load-bearing geometries, enhance aerodynamic performance and reduce material usage while maintaining structural integrity—an advantage for lightweight UAV airframes.

Infill and Cellular Modification

Infill modification in FDM 3D printing allows control over internal density and pattern to tailor mechanical performance. Adjusting infill parameters helps reduce weight, although uniform infill reductions can compromise structural integrity. More advanced strategies, like variable-density infills, offer improved stiffness retention.

Periodic Cellular Structures

Periodic cellular geometries are categorized as 2D (e.g., honeycombs) and 3D (e.g., foams, lattices, syntactic porous structures). [3]Honeycombs offer superior stiffness and energy absorption, while shapes like the diamond core demonstrate consistent elastic and shear moduli with better printability. Kagome lattice structures are particularly promising for UAV wings due to their excellent strength, energy absorption, and crash resistance.

AM Technologies for UAV Manufacturing

A variety of AM techniques are evaluated for UAV applications:

PolyJet: Offers high precision and smooth surfaces, suitable for bio-mimetic microstructures, but lacks sufficient strength for load-bearing UAV structures.

Stereolithography (SLA): Suitable for intricate, lightweight components. However, limited long-term strength and post-processing requirements restrict its use for major load-bearing parts.

Selective Laser Sintering (SLS): Commonly used in UAV fabrication due to its self-supporting nature and reusability of powder. It enables complex geometries, though surface roughness often necessitates post-processing.

Fused Deposition Modeling (FDM): Cost-effective and suitable for prototyping. Layer adhesion, print orientation, and cooling rates significantly affect structural quality. Reinforcements with carbon rods or frames are often employed.

Molten Metal Fusion: Offers dense, strong parts with minimal porosity, but higher material density reduces its suitability for lightweight aerial vehicles.

Electron Beam Melting (EBM): Enables high-quality metal printing with reduced residual stress, but is constrained by material cost, grain size, and build volume limitations.

Laminated Object Manufacturing (LOM): Limited by directional strength variation and non-reusability of support materials, making it less ideal for UAV structures.

Key Considerations for AM in UAV Airframe Design

Strength-to-Weight Ratio: Critical for endurance, maneuverability, and payload capacity. Metal AM offers strength, while plastics favor weight reduction.

Material Homogeneity: Anisotropy and non-uniform strength distribution in printed parts must be addressed in design.

Support Removal: Surface finish is crucial, especially on aerodynamic surfaces. Techniques minimizing or eliminating support structures are preferable.

Build Volume and Scalability: Print bed size influences part segmentation and assembly. FDM and SLS are more suitable for larger UAV components.

Production Volume: AM is cost-effective for low-volume production due to the absence of tooling.

Geometry Complexity: AM enables fabrication of complex, topology-optimized and bio-inspired structures unachievable with conventional methods.

On-Demand Manufacturing: AM supports localized, just-in-time production, reducing logistics costs.

Material and Process Reliability: Variability in material properties (e.g., moisture sensitivity, powder quality) and process parameters affect consistency. Standardization remains an ongoing challenge for critical aerospace applications.

Table 2.2 A brief summary evaluation of AM methods for UAV Manufacturing.

Process	**Resolution**	**Materials**	**Material Type**	**Support**	**Remarks**
FDM	±0.197 mm	ABS, PLA, Nylon & some other thermoplastics	Filament	Soluble or breakaway thermoplastic material	Moderate material strength Moderate surface roughness Feasible impact resistance Layer separation problems Stair stepping problems Variable cost of materials Acceptable resolution **Widely used for UAVs**
SLS	±0.381 mm	Carbon fiber, nylon, plastics, metal, ceramic,glass	Powder	Self–supported	Easy removal of support material High material strength Cost–efficient input material Comparably lower resolution High surface roughness Extensive post–processing Minimal waste

					High demand for initial input material **Widely used for UAV structures** **Widely used for functional part manufacturing**
SLA	± 0.05 mm	Photopolymers	Liquid resin	Liquid resin	Feasible surface quality Break–away support material Loss of material strength over time Time–consuming curing process Post–heat treatment to strengthening Cost–inefficient resin–based material High demand for initial input material Fragile against loading responses **Unfavorable for UAV manufacturing** **Favorable for simple component manufacturing**
LOM	±0.203 mm	Paper, wood, plastic,metal	Sheets	Self–supported	Adhesive dependent quality Layer separation problem Cost–efficient input material Dimensional accuracy problems Tough support removal process

					Inefficient for UAV manufacturing
MJM	±0.076 mm	Acrylic (liquid) plastics	Liquid	Soluble or dissoluble wax–based support	Feasible surface quality High resolution Expensive input material Plastic deformation Suitable for multi–material process Fragile against loading responses **Unfavorable for UAV manufacturing** **Favorable for component manufacturing**

2.4 Quasi-Steady and Unsteady Aerodynamic Forces and moments with transition flight control.

Flight Phases of a Fixed-Wing VTOL UAV

A VTOL UAV (Vertical Take-Off and Landing Unmanned Aerial Vehicle) has multiple flight stages:

1. Vertical take-off and hover
2. Transition to forward flight

3. Backward transition to hover
4. Landing

The **transition phases** are tricky because **aerodynamic forces change rapidly**. These changes are hard to predict using basic models.

[4]Traditionally, researchers assumed **quasi-steady aerodynamics**, which simplifies unsteady effects and uses precomputed data or curve fitting (like CFD simulations or wind tunnel tests). Tools like **XFLR5 or DATCOM** give fast but less accurate results.

But this approach ignores **unsteady aerodynamic effects**, which are crucial during quick transitions. So, **more accurate models** like:

- **CFD (Computational Fluid Dynamics)** — very accurate, but slow and resource-heavy.
- **Unsteady vortex lattice methods** — good for 3D modeling but still demanding.
- **Lumped vortex models** — simpler and used for helicopter blades; can also work well here.

Transition Flight Control

Control during transition is **the hardest part** of VTOL flight. This is because:

- Aerodynamic forces **change rapidly**.
- A **single simple control model** doesn't work throughout the transition.

Traditional (Model-Based) Methods:

- Commonly use **PID controllers**, sometimes with **gain-scheduling**.
- Simplify things by using fewer control surfaces or only using thrust.
- Advanced strategies include:
  - Nonlinear dynamic inversion
  - Trim manifold techniques
  - Control mixing (rotor + control surfaces)
  - Switching between different models during flight
  - Output regulation for disturbance handling

Handling Complexities:

- Some researchers try to **mathematically model** unexpected changes like:
  - Shift in **center of gravity**
  - Errors in aerodynamic estimates
- Techniques like **backstepping** offer stability but are math-heavy.

Model-Free Controllers (Less Common but Promising)

These don't depend on precise models:

- **Artificial Neural Networks (ANNs)** are used to help traditional controllers (like PID) adapt to changes and disturbances.
- ANNs also help reduce the need for complex tuning.
- **Fuzzy Logic Controllers (FLC)** handle disturbances well and can be improved further with ANN — resulting in **Fuzzy Neural Networks (FNNs)**.
  - **Type-2 FNNs (T2FNN)** are better in noisy or unpredictable environments than Type-1.
  - These allow learning and adapting during flight.

In Summary:

- Accurate modeling of transition flight is crucial but challenging due to unsteady aerodynamics.
- Traditional control methods work but struggle with changing dynamics.
- Hybrid approaches (ANN + PID/FLC) can adapt better but are more complex.
- Type-2 Fuzzy Neural Networks show promise for future adaptive control systems in full VTOL flight.

Chapter-3

DESIGN AND MANUFACTURING

3.1 FE Model of the UAV

The dynamic responses of the UAV are neglected and a quasi-equilibrium condition is assumed. [5]The loads on the UAV structure are computed for a single maximum load case of 3, which is a safe value to consider. A factor of safety of 1.5 is included in the calculation of the loads. The aerodynamic loads are computed using XFLR5. The aerodynamic loads are given in the FE model as cut-loads which comprise three orthogonal pairs of shear force, bending moment, and torsional moments acting on the elastic axis along the span of the UAV.

The shear force, bending moment, and the torsional moment are applied using the structural distributing elements. Inertial relief loads, such as the mass of the motors, motor booms, battery etc., are applied as a point mass in the FE model. A fixed boundary condition is employed at the plane of the symmetry of the model as the wing is approximated as a cantilever beam fixed to the mid-rib.

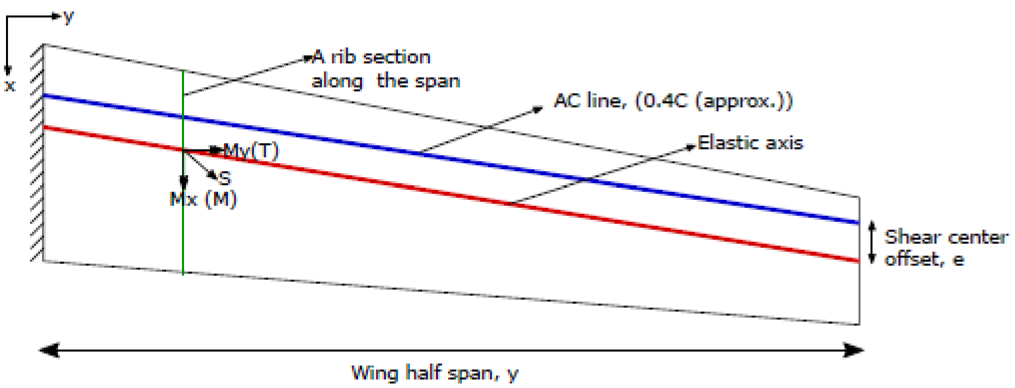

Figure 3.1: A representative location of elastic axis and cut loads applied along wing

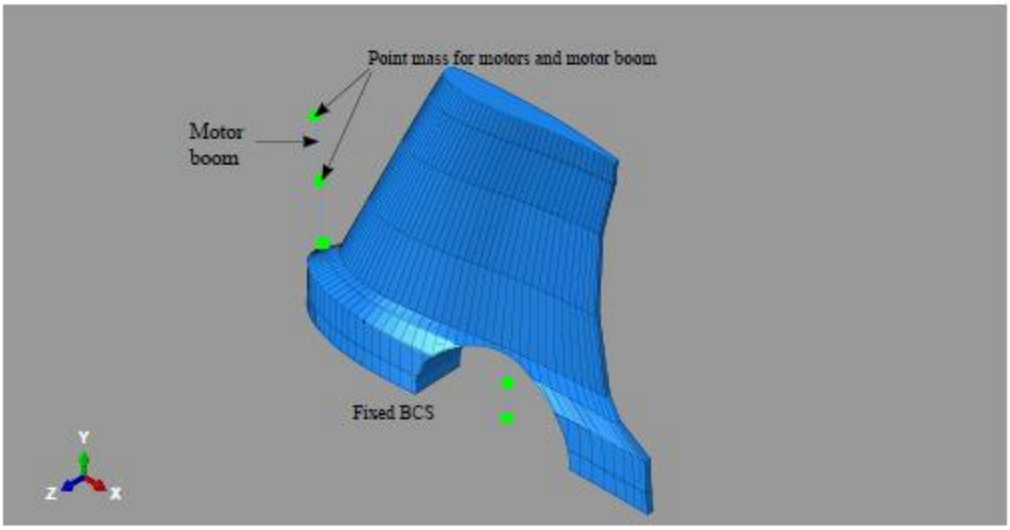

Figure 3.2: Point mass and boundary conditions in FE model.

Number of ribs	Element type	
	S4R	B31 (158-front, 125-rear)
9	83189	283
11	85071	283
13	85488	283

Table 3.1: Number of elements in the final FE model after the mesh convergence test.

The mechanical properties from Table 3.1 are used as input to the software. The FE model created in ABAQUS includes the skin and ribs meshed with a 4-node shell element, S4R, and the motor booms meshed using the two-node linear beam element, B31. Three FE models are created with varying number of ribs depending upon the combinations mentioned in the L9 orthogonal array.

Analysis no.	Sheet thickness	No. of ribs	Build Orientation	von Mises (MPa)	Mass (kg)	S/N von Mises	S/N Mass
1	**0.5**	**9**	**EU**	**8.342**	**0.889**	**-18.425**	**1.022**
2	0.5	11	FU	9.742	1.010	-19.773	-0.086
3	0.5	13	SU	10.760	1.160	-20.636	-1.289
4	**0.75**	**9**	**FU**	**5.239**	**0.999**	**-14.385**	**0.009**
5	0.75	11	SU	6.100	1.120	-15.707	-0.984
6	0.75	13	EU	6.592	1.270	-16.380	-2.076
7	**1**	**9**	**SU**	**3.310**	**1.110**	**-10.397**	**-0.906**
8	1	11	EU	3.820	1.230	-11.641	-1.789
9	1	13	FU	3.944	1.380	-11.919	-2.798

Table 3.2: The L9 orthogonal array, response values from FE simulations and the S/N values for the responses recorded.

[5]The Taguchi method based on the L9 orthogonal array is conducted to provide a simple, computationally cost-effective and systematic method for determining the optimum level of the controllable factors.

The highlighted values in the tables show the optimum values that could be chosen for the least weight and best mechanical performance of the UAV. A low-stressed structure is possible if the skin thickness, the number of ribs and the build orientation are 1 mm, 9, and FU respectively. For the least structural mass, these factors must take the values of 0.5 mm, nine ribs, and EU orientation. Without exception, both the responses demand a maximum rib quantity of 9.

Therefore, between the configurations considered, the one corresponding to the analysis with 0.75 mm skin thickness, 9 ribs, and FU orientation is the least stressed and has a structural mass close to the value used in stability and aerodynamic analysis. Hence, this combination can be chosen as the most optimum for the fabrication of the initial prototype.

3.2 Sizing of Key Performance Parameters and CAD Model of the UAV

1. Aircraft Parameters

Wingspan	2021 mm
Wing Area	3684 cm^2 (0.3684 m^2)
Maximum Takeoff Weight	6kg
Cruise Speed	45–65 km/h (12.5–18 m/s)
VTOL and Pusher prop Diameter	13 inches
Power Efficiency	2 Wh/km

2. Stall Speed Calculation

Using the lift equation:

$$V_s = \sqrt{\frac{2W}{\rho S C_L}}$$

Where:

- $W = 6 \times 9.81 = 58.86\,\mathrm{N}$
- $\rho = 1.225\,\mathrm{kg/m^3}$
- $S = 0.3684\,\mathrm{m^2}$
- $C_L = 1.2$

$$V_s \approx \sqrt{\frac{117.72}{0.541}} \approx 14.8\,\mathrm{m/s} \approx 53.3\,\mathrm{km/h}$$

2. Required Thrust for Hover (VTOL Mode)

You must produce **more than total weight** with vertical thrust.

$$\text{Total Thrust} \geq W = 6 \times 9.81 = \boxed{58.86\,\mathrm{N}}$$

Assume **4 VTOL motors**:

$$\text{Thrust per motor} = \frac{58.86}{4} \approx \boxed{14.7\,\mathrm{N/motor}}$$

Each VTOL motor + 13” prop must deliver **at least 15 N** of thrust at full throttle (with some headroom, target 18–20 N).

4. Motor and Propeller Sizing

To check whether a **13-inch prop** is good for VTOL:

- A typical 13x4.4 prop on a **6S setup with 700–900 kV motors** produces ~2.2–2.5 kgf of thrust (~21–25 N).

- Your requirement (15 N) is **well within range**.

Same for **pusher prop** at 13” – more than enough to sustain cruise and push the UAV.

5. Battery Sizing for Mission

Say you want:

- **45 mins of flight** at cruise (108 W)
- Add 2 minutes VTOL operation at **300 W** per motor × 4 = 1200 W

Energy required:

Cruise:

$$108 \times \frac{45}{60} = 81\,\mathrm{Wh}$$

VTOL (takeoff + landing):

$$1200 \times \frac{2}{60} = 40\,\mathrm{Wh}$$

Total = 81 + 40 = 121 Wh

Add 20% safety margin:

145Wh

Battery options:

- 4S 10000 mAh = 14.8 V × 10 Ah = 148 Wh
- 6S 6000 mAh = 22.2 V × 6 Ah = 133 Wh (just below)

A 4S 10Ah pack is ideal **for this mission profile.**

5. Power and battery Requirements

Assume:

- Cruise power = 108 W
- VTOL power = 1200 W (4 × 300 W motors)

Mission Profile:

- Cruise duration: 45 minutes

$$108 \times \frac{45}{60} = 81 \text{ Wh}$$

- VTOL (2 mins):

$$1200 \times \frac{2}{60} = 40 \text{ Wh}$$

Total Energy Required = 121 Wh

Add 20% safety buffer ⇒ **~145 Wh**

Use **4S 10,000 mAh** battery (148 Wh)

5. Estimated range

Efficiency = 2 Wh/km

Total energy = 145 Wh

$$\text{Range} = \frac{145}{2} = \boxed{72.5\,\text{km}}$$

Maximum range ≈ **72.5 km**

9. Analysis and Discussion

The performance assessment of the UAV platform was conducted to evaluate its aerodynamic and energy efficiency, as well as to ensure its structural and propulsive feasibility under typical mission conditions. The calculations considered essential flight parameters, such as cruise and stall speeds, required thrust, and energy consumption based on a conservative and realistic mission profile.

The stall speed was calculated to be approximately **14.8 m/s (53.3 km/h)**, which falls within the safe margin considering the intended cruise range of **45–65 km/h**. This confirms the aerodynamic design is capable of maintaining stable flight even near the lower bounds of the speed envelope, which is crucial for loitering and precision missions such as surveillance or mapping.

During cruise, the required thrust was found to be **~1.76 N**, which is comfortably achievable with a pusher configuration using a 13-inch propeller paired with a high-efficiency electric motor. The relatively low cruise thrust requirement is indicative of an efficient aerodynamic configuration, contributing to extended range and reduced power consumption.

Vertical take-off and landing (VTOL) performance was also assessed, showing a total thrust requirement of approximately **58.86 N**, translating to **~15 N per motor** assuming a quadrotor lift setup. This requirement is well within the capabilities of motors equipped with 13x4.4 propellers, commonly capable of generating over **20 N** of thrust each under 4S–6S operation.

From a power systems perspective, the cruise power was estimated to be **~108 W**, while short-duration VTOL operations demand significantly higher power (**~1200 W** for 2 minutes). Factoring in a 20% energy buffer, a **4S 10,000 mAh LiPo battery** (approx. 148 Wh) was deemed suitable, balancing the needs for endurance and payload without exceeding weight limitations. This configuration supports an estimated flight range of **~72.5 km**, assuming 2 Wh/km energy efficiency, enabling practical medium-range applications.

The UAV design achieves a strong trade-off between structural weight, propulsion efficiency, and energy autonomy. These calculations validate the feasibility of the selected design parameters, ensuring that the aircraft remains within both performance and operational bounds across various flight segments, including VTOL, transition, and cruise phases.

Wing Configuration for PHOENIX Platform

The initial conceptualization of the PHOENIX fixed-wing VTOL platform explored the use of a tailless configuration inspired by the Fauvel AV series. This design was considered due to its compact layout and potential aerodynamic efficiency. However, after iterative simulations and comparative studies, it was determi.ned that the Fauvel-inspired tailless wing was not the most optimal choice.

Among the wing configurations tested, the compound wing using NACA 2412 and NACA 4412 airfoils emerged as the most suitable choice for the PHOENIX VTOL platform. While the Fauvel-inspired tailless configuration initially appeared promising due to its inherent stability characteristics, further comparative studies revealed that the compound wing delivered superior performance in terms of lift-to-drag ratio, structural simplicity, and modular adaptability for fixed-wing VTOL integration. A detailed aerodynamic and structural analysis justifying this selection will be presented further in the document.

The compound wing offers a hybrid airfoil distribution along the span—utilizing NACA 2412 near the root and transitioning to NACA 4412 towards the tips. This setup aids in optimizing lift distribution and delay of stall, which are critical for both vertical and horizontal flight regimes. The high camber of the 4412 airfoil contributes to enhanced lift during VTOL operations, while the moderate camber of the 2412 airfoil provides stability and efficiency during cruise.

Moreover, this configuration facilitates better mounting options for tilt-rotor mechanisms, as well as internal compartmentalization for battery and avionics modules. The improved manufacturability of this wing design using composite materials and FDM 3D printing methods also contributes to its feasibility in rapid prototyping and testing scenarios.

Overall, the compound wing design presents an optimal trade-off between performance, structural integrity, and ease of integration with the VTOL system, making it the most viable option for the PHOENIX platform going forward.

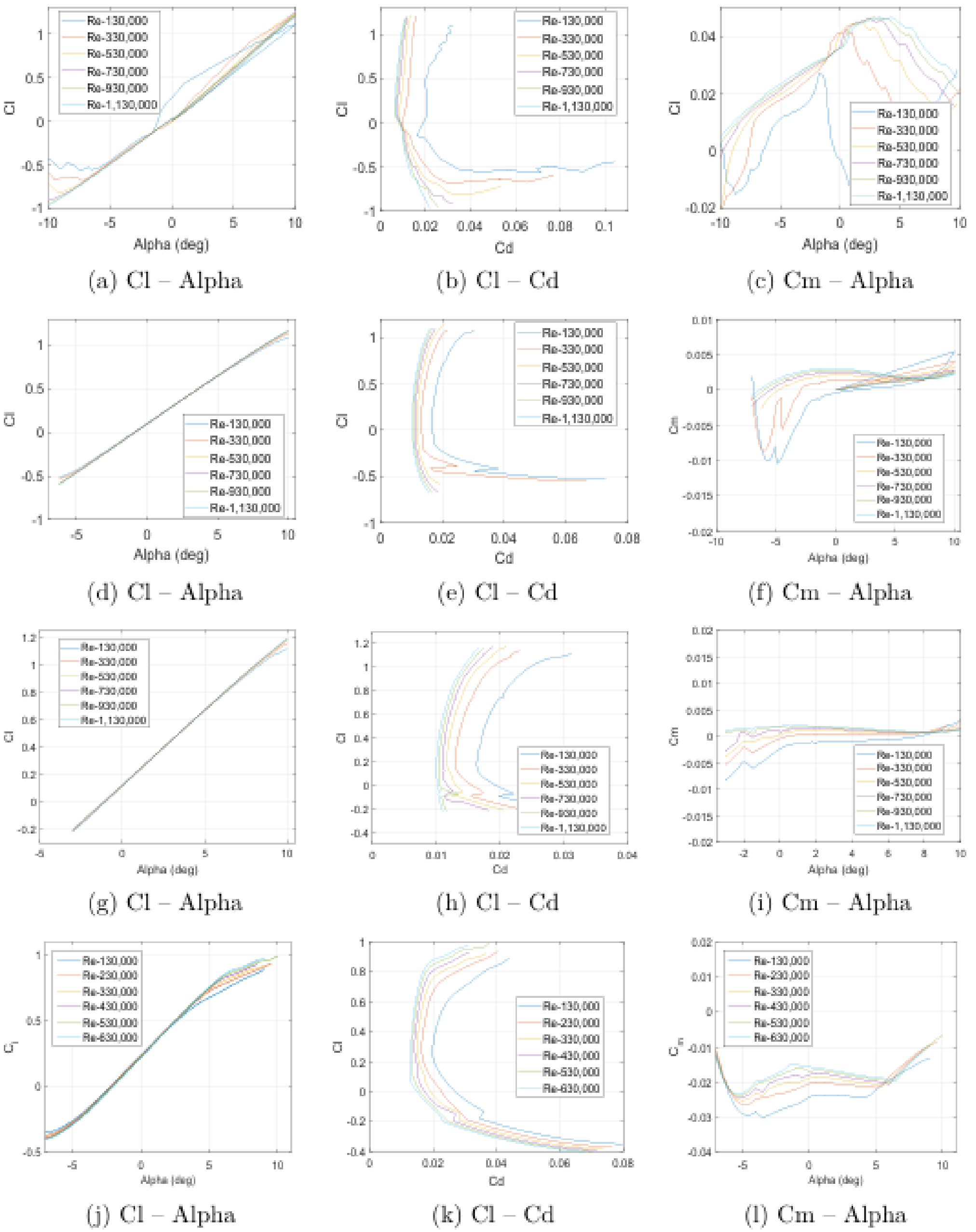

Figure 3.3: AirfoilcharacteristicsforFauvel(a),(b),(c);S5010(d),(e),(f);S5020(g), (h), (i);andWortmannFX05-H-126(j), (k), (l).

Computer Aided Design of the Unmanned system

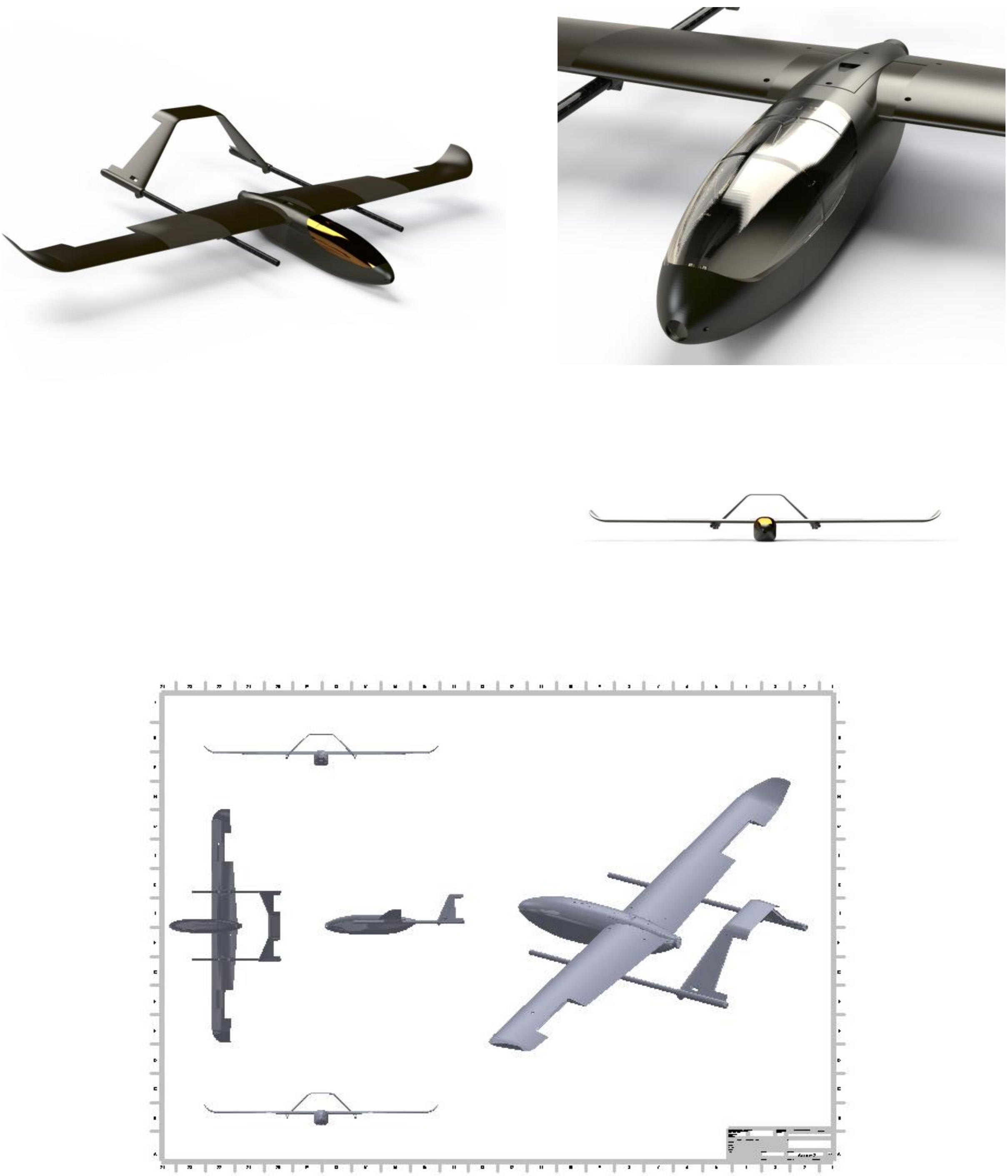

Figure 3.3: CAD and rendered model of the Unmanned Aerial Vehicle

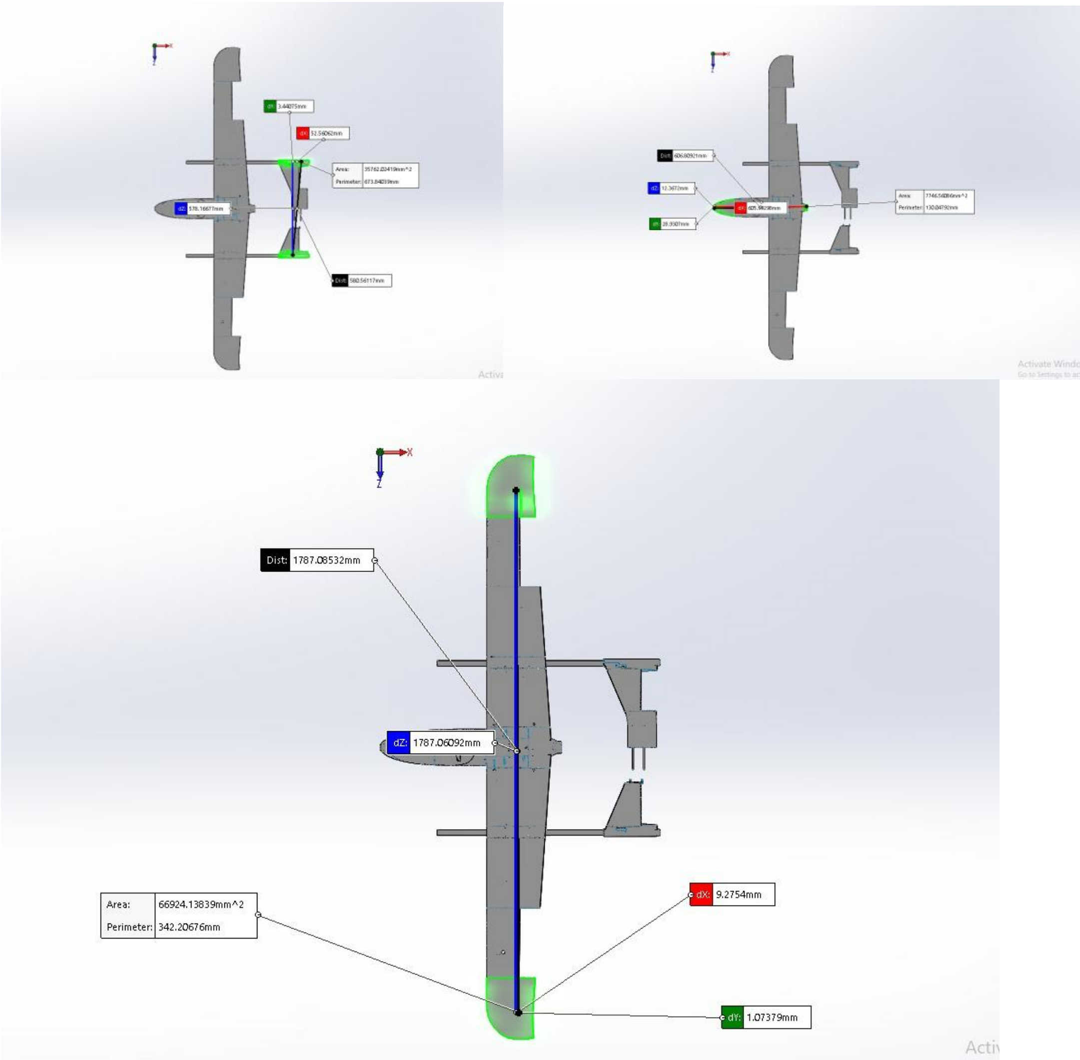

Figure 3.3: CAD model with evaluated data of wing span and fuselage span

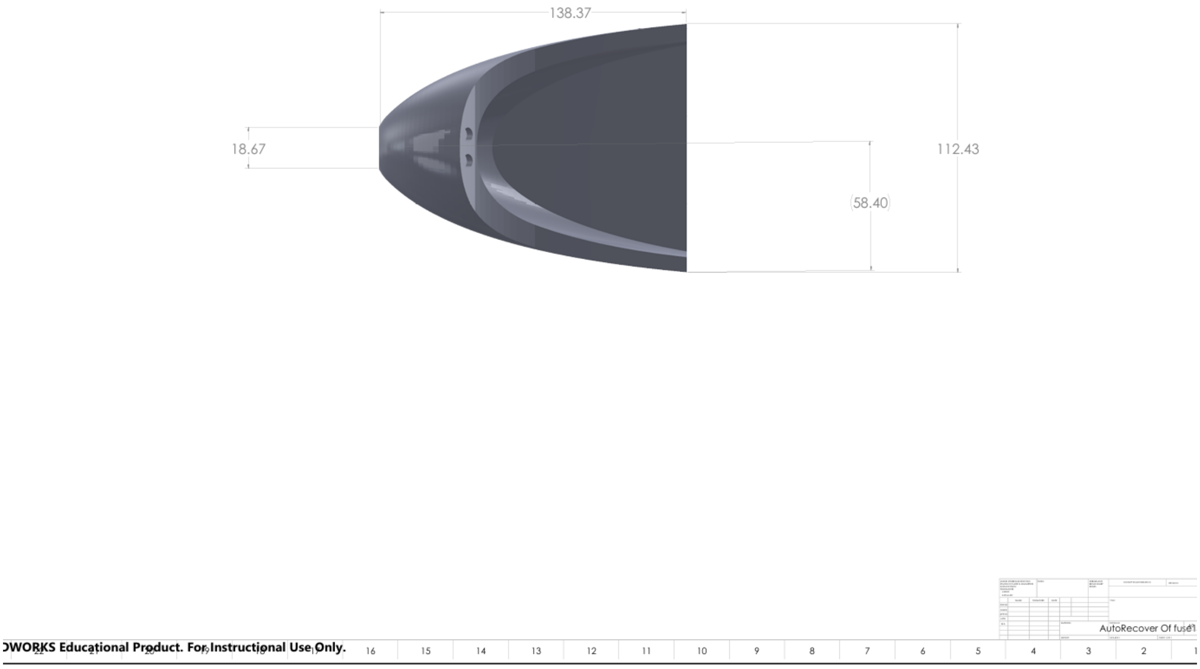
138.37
18.67
112.43
(58.40)
AutoRecover Of fuse1
DWORKS Educational Product. For Instructional Use Only.

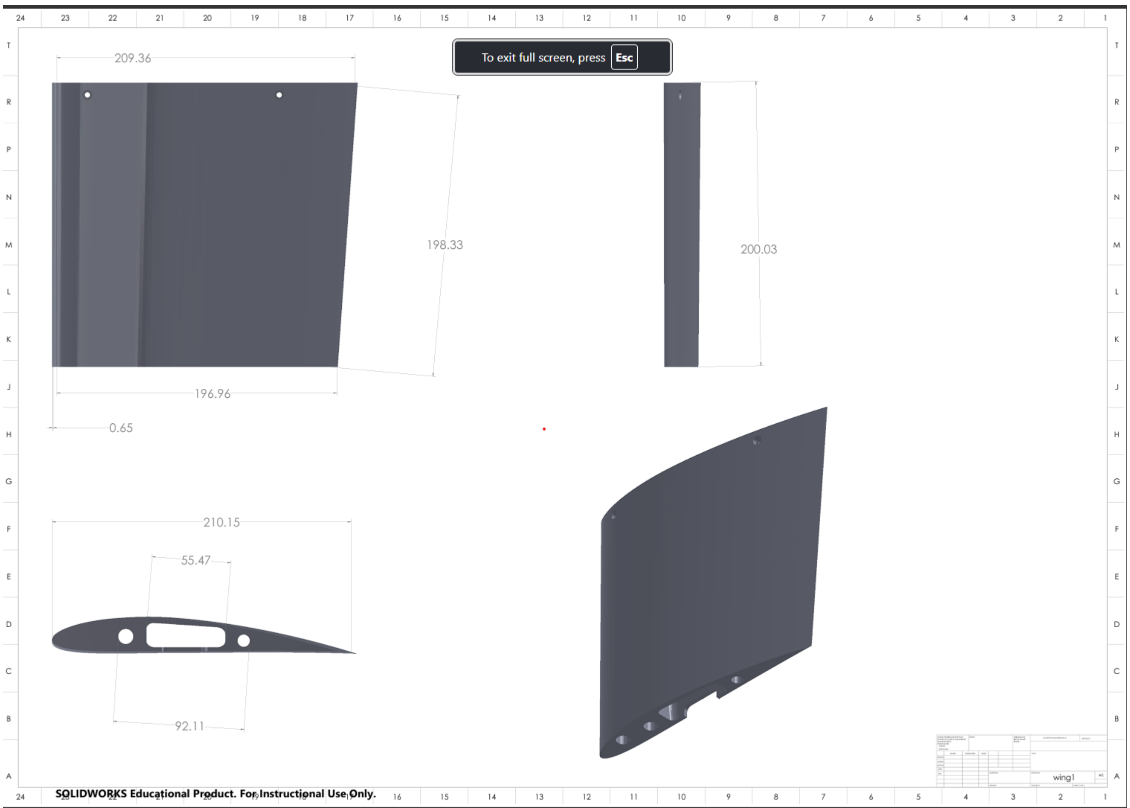
To exit full screen, press Esc
209.36
198.33
200.03
196.96
0.65
210.15
55.47
92.11
wing1
SOLIDWORKS Educational Product. For Instructional Use Only.

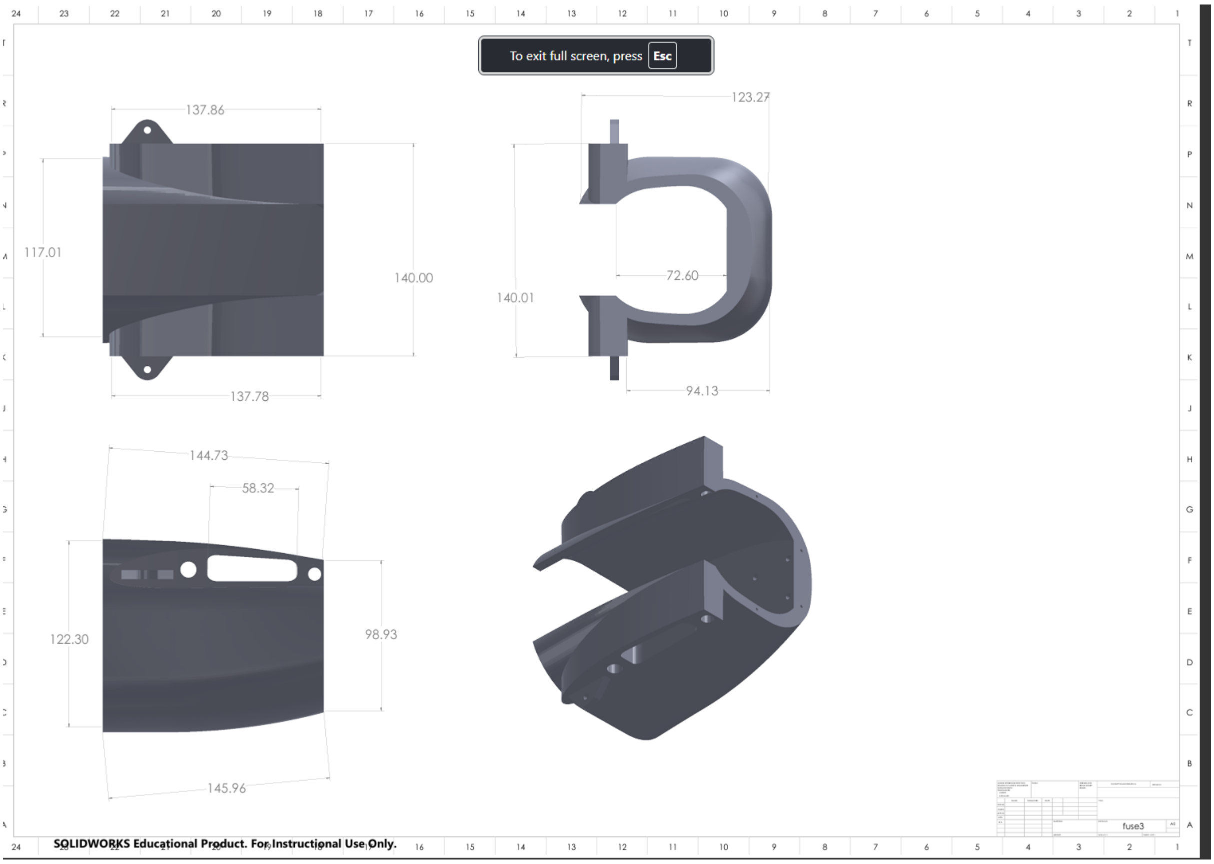

Figure 3.4: Drawing files with dimensions of segmentised parts of the UAS

Chapter-4

COMPUTATIONAL FLUID DYNAMICS ANALYSIS

4.1 Introduction

The results obtained from CFD are compared to XFLR5 to determine whether XFLR5 is reliable. XFLR5 simulations are unable to predict values after 15° for U=20m/s and after 10° for U=5m/s. Figures C.1a and C.1b show that CL and CD obtained from CFD simulation are constantly higher than XFLR5 simulations. CLα from CFD and XFLR5 are similar. XFLR5 results are independent of flow velocity, whereas CFD has some Re variability as seen from the plots. Stall is not possible in XFLR5. XFLR5 underestimates CD when compared to CFD. Figure C.1c shows that Cm curve obtained from XFLR5 trims at a high angle but the plots that were obtained from CFD have lower trim angles. Cmα for CFD and XFLR5 are different. Cm obtained from XFLR5 does not have a large difference with varying velocities at the same α. However, CFD shows that Cm values have a larger difference in values when velocity is varied at the same α. XFLR5 is also unable to simulate for the increase in Cm after stall angles

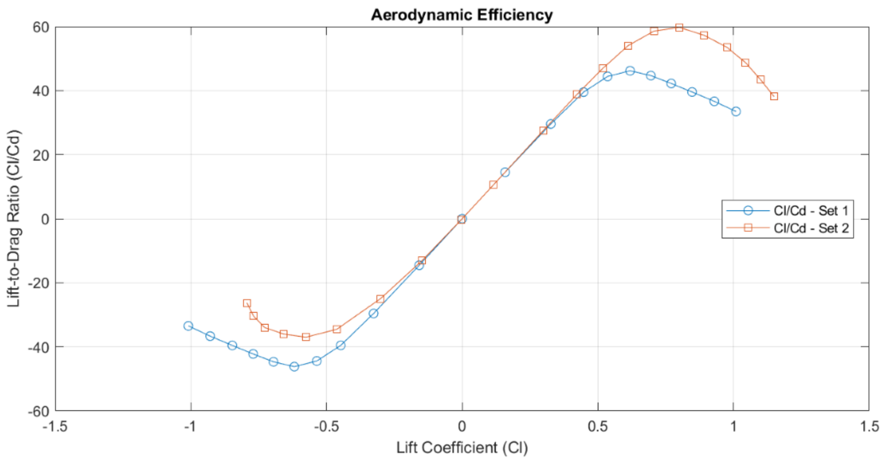

(a) cl/cd vs cl

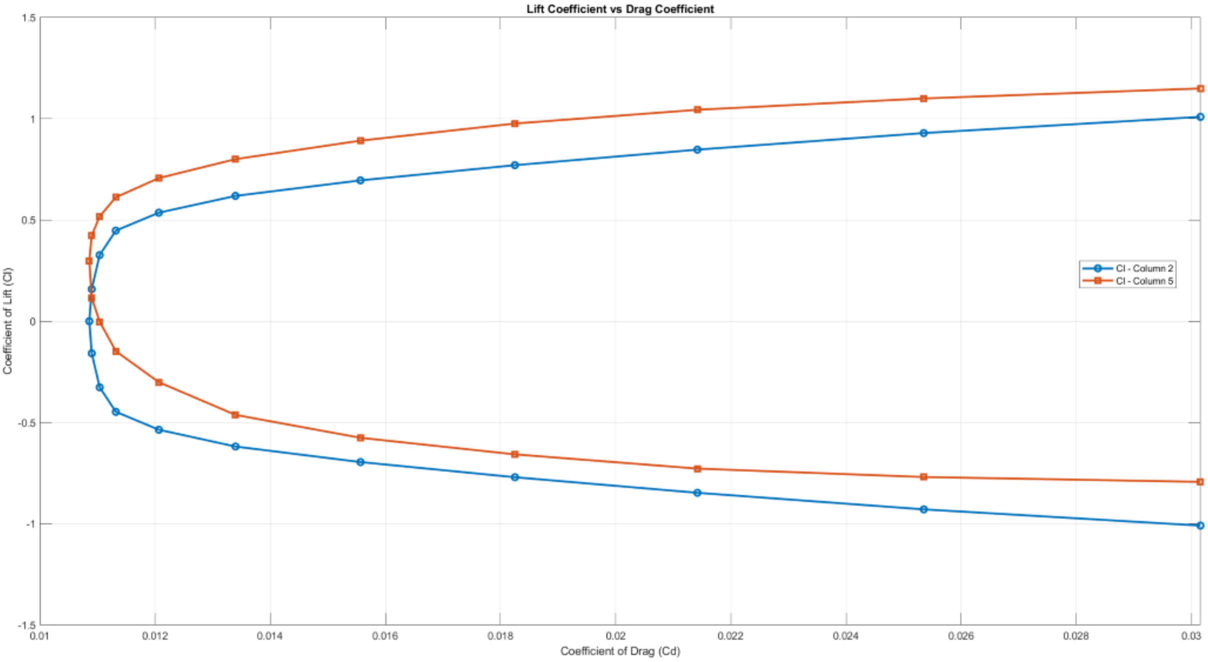

(b) NACA 2412 and NACA 0012 performance parameters

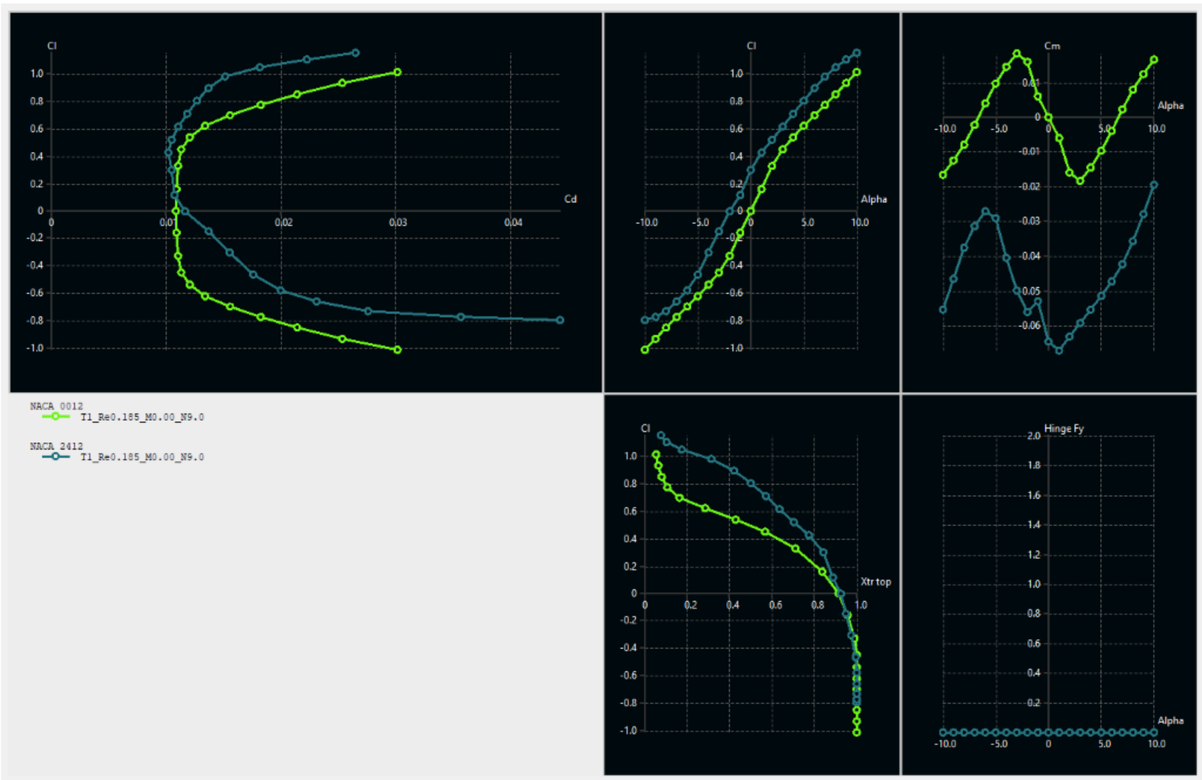

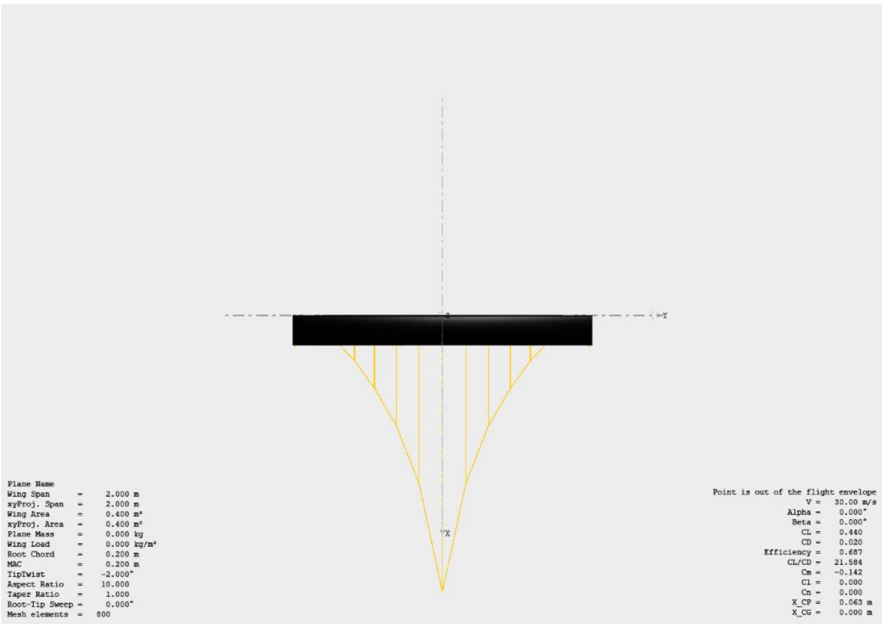

(c) Wing Planform Design

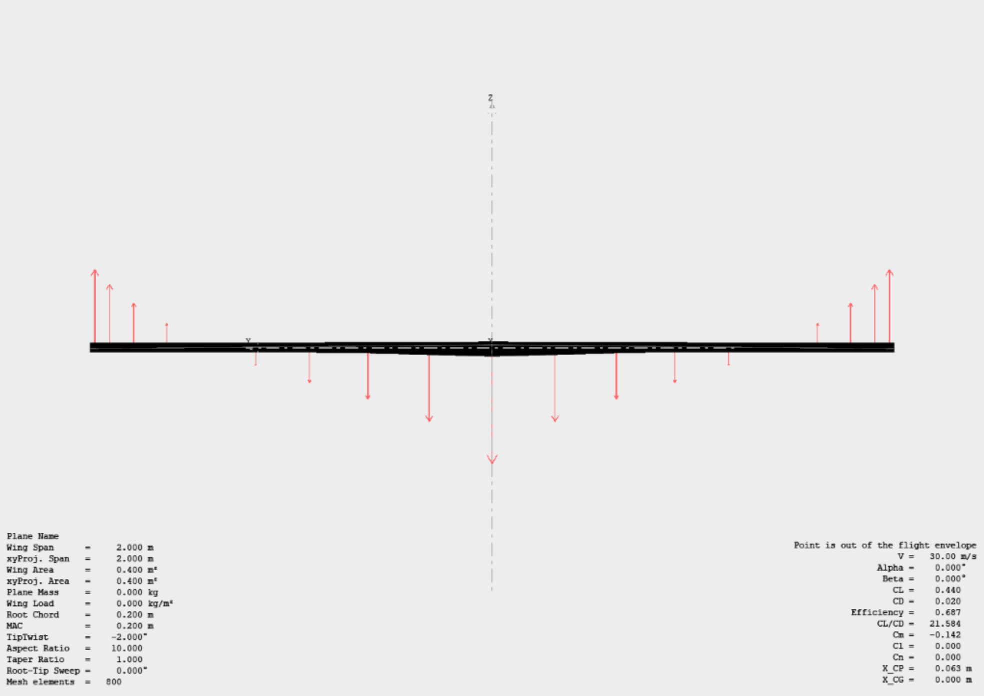

(c) Wing Planform Design

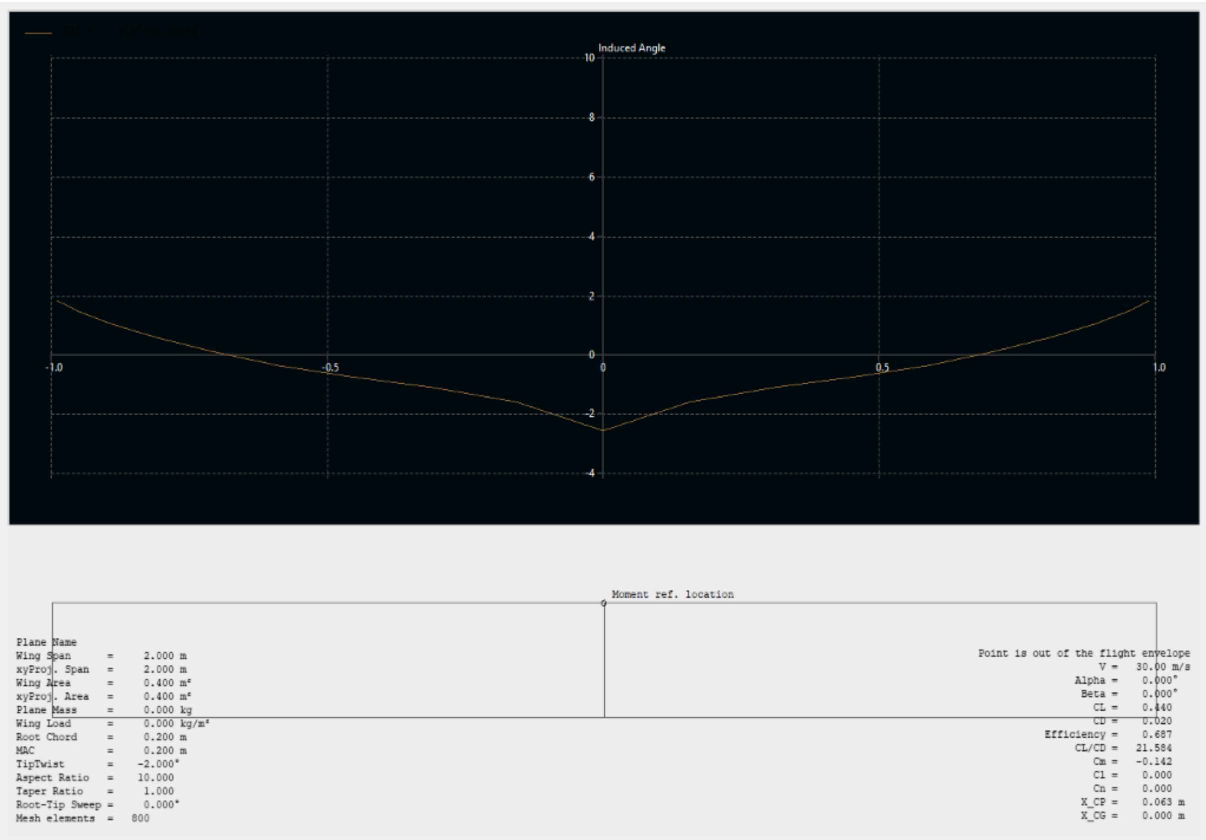

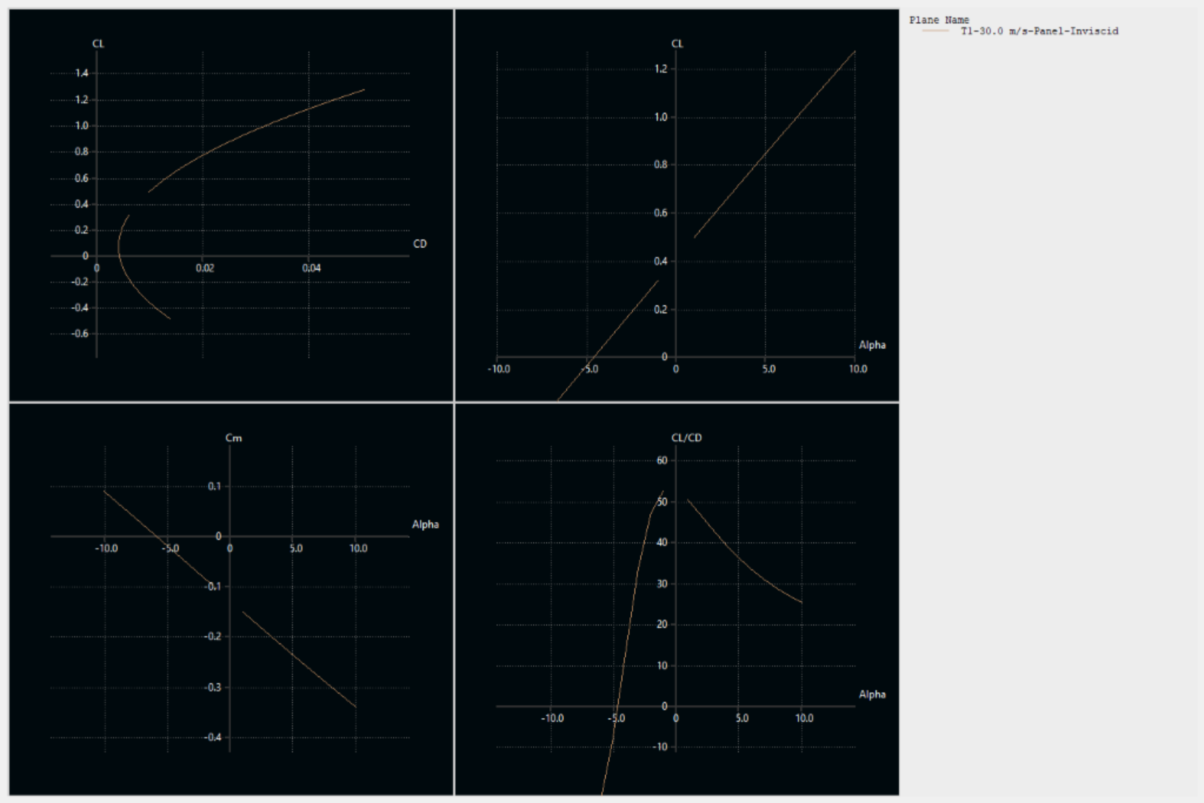

Figure (a) A comparative analysis between the two airfoil configurations reveals that Set 2 significantly outperforms Set 1 in terms of aerodynamic efficiency, as indicated by the lift-to-drag ratio (Cl/Cd). Set 2 reaches a peak Cl/Cd of approximately 55, while Set 1 achieves a maximum closer to 45. This higher efficiency of Set 2 makes it particularly advantageous for sustained forward flight, where minimizing drag relative to lift is essential for conserving energy and improving endurance.

The efficiency peak for Set 2 occurs around a Cl value of 1.0, which likely corresponds to the optimal angle of attack during cruise conditions. Operating near this Cl during level forward flight would maximize performance, particularly in battery-powered platforms where energy management is crucial.

Moreover, the Cl/Cd curve for Set 2 is symmetrical around Cl = 0, indicating a smooth transition between negative and positive lift regions. This characteristic is especially beneficial for flight regimes involving maneuvering, hover, or bidirectional flow, and further supports the use of symmetrical or semi-symmetrical airfoils in such applications.

However, the analysis also reveals a steep decline in Cl/Cd following the peak, a typical sign of stall behavior at high angles of attack. This underscores the importance of avoiding operation just past the efficiency peak during transitions, as doing so may lead to aerodynamic stall and subsequent instability.

Finally, the region of negative Cl exhibits markedly low and even negative Cl/Cd values, suggesting a significant drag penalty in those conditions. This portion of the curve is generally inefficient and not desirable for standard flight unless inverted or unconventional orientations are explicitly required.

Based on this analysis, Set 2—comprising a compound wing derived from the NACA 2412 and NACA 4412 airfoils—emerges as the superior choice. Although the Fauvel-inspired configuration was initially considered, the compound wing offers better overall performance for the mission profile, and a detailed justification for this selection is presented in subsequent sections.

Figure (b)

Cl vs. Cd Behavior Analysis

The general trend observed in the Cl vs. Cd plot aligns with expected aerodynamic behavior, where the coefficient of lift (Cl) increases alongside the coefficient of drag (Cd). The curve spans both positive and negative regions of angle of attack (AoA), with the upper portion corresponding to positive AoA and the lower portion representing negative AoA values. The narrow "pinched" region near the center of the curve denotes the point of minimum drag, which typically signifies the most efficient condition for cruising flight.

For Set 1 (corresponding to the blue curve in Column 2), the aerodynamic performance peaks around a Cl value of 1.0 with a corresponding Cd of approximately 0.018. This configuration generates lower lift and exhibits more drag in comparison to Set 2, suggesting it represents a more conventional or baseline airfoil configuration with limited optimization.

In contrast, Set 2 (represented by the red curve in Column 5) demonstrates superior aerodynamic characteristics across nearly the entire range of Cd values. It achieves higher lift for a given drag and reaches a greater maximum Cl, albeit at a slightly higher drag coefficient. This performance indicates a more refined or aerodynamically advanced design. The enhanced lift characteristics, combined with relatively modest increases in drag, make

Set 2 more suitable for high-efficiency applications where lift-to-drag ratio is critical.

This analysis supports the conclusion that Set 2, generated using a compound configuration derived from the NACA 2412 and NACA 4412 airfoils, offers better overall aerodynamic performance than the initially considered Fauvel-inspired configuration. A detailed justification for adopting this compound wing design is provided in later sections of the report.

Figure (c)

1. Cl vs Cd (Lift-to-Drag Performance)

NACA 2412 demonstrates higher maximum lift and lower drag across the operational envelope, resulting in a superior lift-to-drag (Cl/Cd) ratio. This makes it more efficient for forward flight phases such as cruise and transition.

Preferred airfoil: NACA 2412

2. Cl vs AoA (Lift Behavior)

NACA 2412 has a steeper lift slope, higher maximum Cl, and delayed stall angle, making it suitable for lift-intensive phases like take-off and climb. NACA 0012 offers balanced and predictable performance, especially in symmetrical flow conditions such as hover.

Lift performance: NACA 2412

Hover stability: NACA 0012

3. Cm vs AoA (Pitching Moment Behavior)

NACA 0012 exhibits near-neutral pitching moment characteristics, reducing the need for trim adjustments—advantageous in hover and low-speed control. NACA 2412 introduces a nose-down moment, requiring active trim or elevator compensation.

Trim and pitch stability: NACA 0012

4. Laminar-to-Turbulent Transition (Xtr)

NACA 2412 maintains laminar flow over a greater surface length on both the upper and lower sides of the airfoil, resulting in reduced skin-friction drag and improved aerodynamic efficiency.

Boundary layer efficiency: NACA 2412

5. Control Surface Hinge Force (Fy vs AoA)

NACA 2412 shows stable and consistent hinge force trends, enabling predictable control surface actuation. Data for NACA 0012 hinge forces is limited.

Control predictability: NACA 2412

Figure (d)

Lift Distribution Analysis of Compound Wing (NACA 2412 + NACA 0012)

The lift distribution along the span of the compound wing, derived through Lifting Line Theory (LLT) analysis in XFLR5 at a freestream velocity of 30 m/s, demonstrates a smooth, near-elliptical profile. The central portion of the wing, likely utilizing the cambered NACA 2412 airfoil, shows a peak in lift generation, contributing significantly even at zero degrees angle of attack. This behavior is characteristic of cambered sections, which generate positive lift under symmetric flow conditions. As the analysis moves outward along the span, the lift contribution gradually diminishes, approaching near-zero values at the tips—consistent with the use of the symmetric NACA 0012 airfoil that does not produce lift at zero incidence. This progressive reduction in lift indicates a well-blended transition between airfoil sections, with no apparent aerodynamic discontinuities.

The overall lift coefficient (CL = 0.140 at $\alpha = 0°$) and center of pressure location (X_CP = 0.063) suggest the aerodynamic center is slightly forward, typical for configurations using a forward-cambered section like the NACA 2412. The smooth lift profile enhances aerodynamic efficiency by approximating an ideal elliptical distribution, thereby minimizing induced drag. However, the asymmetry in pitching moment due to the cambered center section introduces a nose-down tendency, which may necessitate control surface compensation or trim adjustments. Furthermore, while the NACA 0012 tips offer improved stability and reduced pitching moment, they contribute little to lift under cruise conditions, potentially underutilizing the span.

This design strategy is especially favorable in hybrid aircraft, such as VTOL systems, where the cambered center provides necessary lift during forward flight, and the symmetric tips enhance pitch neutrality and hover stability. Although the current wing lacks geometric twist, implementing washout could further refine tip behavior and delay stall. Overall, the compound configuration reflects a thoughtful aerodynamic compromise between lift performance and control stability across multiple flight regimes.

Figure (e)

Induced Drag Distribution Analysis of Compound Wing (LLT Method)

The compound wing configuration employing a NACA 2412 airfoil at the root and a symmetric NACA 0012 airfoil at the tips demonstrates a distinct induced drag distribution when analyzed using Lifting Line Theory (LLT) in XFLR5 at a freestream velocity of 30 m/s and zero degrees angle of attack. The induced drag is highest near the mid-span, where the cambered NACA 2412 airfoil dominates and contributes significantly to lift generation. As expected, the induced drag progressively diminishes towards the wing tips, attributed to the symmetric NACA 0012 airfoil that generates minimal lift at this condition. The observed distribution resembles an elliptical curve but deviates slightly due to the absence of geometric twist and the aerodynamic disparity between the center and tip sections.
The overall span efficiency factor (e ≈ 0.687) indicates moderate aerodynamic effectiveness, falling short of ideal efficiency values due to the lack of tapering and washout. The lift-to-drag ratio (CL/CD) of approximately 21.58 further highlights the wing's capability to produce lift with relatively low induced drag. However, design optimizations such as the introduction of geometric twist or spanwise tapering could improve the efficiency by balancing the lift distribution and minimizing tip losses. This configuration suggests a promising balance between lift concentration at the center and drag-reducing effects at the tips, making it suitable for applications requiring enhanced stability and moderate performance, such as VTOL platforms and low-speed UAVs.

4.2 Aerodynamic Center and Center of Pressure, Various Wing Planform

In the study of aerodynamics, understanding the concepts of the center of pressure and the aerodynamic center is essential. [6]The relationship between these points plays a critical role in analyzing an aircraft's stability and control characteristics. Additionally, the variation of the lift coefficient (c_L) with respect to the angle of attack (α) can be effectively modelled through mathematical expressions, providing valuable insights into the aerodynamic behaviour of air foils and lifting surfaces.

We have

$$c_L = c_{L_0} + c_{L_\alpha}\alpha$$

[1]This corresponds to variation of lift coefficient and angle of attack in the linear region of angle of attack. At the same time, we have defined two important parameters. One is aerodynamic center

(ac) the other one is center of pressure (cp). Center of pressure is a point about which resultant aerodynamic forces act and above center of pressure the pitching moment is zero. Aerodynamic center is defined as the point about which pitching moment remains constant with angle of attack.

Let us now consider an airfoil and say xac is the distance of aerodynamic center with respect to the leading edge and x_{cp} is the location of center operation with respect to leading edge here. Now let us take the moment. Let O be the leading edge here and we are going to derive the moment expression about this point O for this particular aerofoil. Say, we are testing it at certain α.
Let us consider there is a flow with a velocity v∞ over this airfoil. When there is a flow there is lift and drag and also there is lift and drag at moment about aerodynamic center. Now let us consider the moment about point O by considering the forces and moment acting at aerodynamic center.

Aerodynamic Center and Center of Pressure

Now the pitching moment about point O,

$$Mo = Mac - xac(L)$$

$$c_m = c_{m_{ac}} - \bar{x}_{ac}(c_L)$$

Where, ;

$$M = \frac{1}{2}\rho v^2 S\bar{C}C_m$$

;

$$L = \frac{1}{2}\rho v^2 S C_L$$

$$\bar{x}_{ac} = \frac{x_{ac}}{\bar{c}}$$

Now if you take the moment about the same reference point by considering the forces acting at the center of pressure (since center of pressure is defined as the point about which the resultant aerodynamic forces act), what we have is the moment due to lift because the drag contribution is very less along the same axis, hence neglecting drag.

So, the pitch down moment due to lift is

$$C_m = \frac{-(x_{cp})}{\bar{C}} C_L$$

$$Cm = -\bar{x}cpCL$$

Above two equations represent the moment about point O due to lift. The moment should be equal whether you are considering with respect to aerodynamic center or center of pressure. By equating those 2 what we have?

$$\bar{x}_{cp} = \bar{x}_{ac} - \frac{C_{m_{ac}}}{C_L}$$

This is the relationship between center operation and aerodynamic center. We also address that at higher angle of attack the C_L increases due to which $\frac{C_{m_{ac}}}{C_L}$ becomes very low and this $\bar{x}_{cp}$ will move close towards $\bar{x}_{ac}$.

Now let us take up an example.
Example:

NACA 2412 airfoil is tested in a low speed wind tunnel. It is observed that the pitching moment coefficient about the leading edge at zero lift is – 0.02. Also, at $\alpha=8^o$ the C_L is measured to be 0.7 and C_m about leading edge is -0.2. Find the aerodynamic center for the airfoil.

Solution:

Given,

$$\alpha = 8^0$$

$$C_L = 0 \cdot 7$$

$$C_{mLE} = -0.2$$

Given C_m about leading edge at C_L=0 is -0.02.

$$C_{m_{LE(c_L=0)}} = -0.02$$

[2]Let us say this is our leading edge and this is my aerodynamic center Let this distance be $x_{ac.}$ V_∞ and α will have lift and moment about aerodynamic center. Now, if you write an equation for pitching moment about aerodynamic center about this leading edge with respect to this aerodynamic center, we have

$$Cm = Cmac - \bar{x}acCL$$

From the above equation,

the moment about leading edge, at $C_L = 0$, measured to be -0.02 turns out to be the moment about aerodynamic center.

$$C_{mac} = -0.02$$

From the same equation we have C_L at α=8 degrees and the corresponding C_m.

By substituting the corresponding values,

$$-0.2 = -0.02 - \bar{x}_{ac} 0 \cdot 7$$

$$\bar{x}_{ac} = \frac{-0.02 + 0 \cdot 2}{0 \cdot 7}$$

$$\bar{x}_{ac} = 0.2571$$

$\bar{x}$ is a non-dimensional number.

$$x_{ac} = 0.2571\bar{C} = 25\% \ \bar{c}$$

Hence, for low speed flight vehicles, the aerodynamic center in general lies at about 22 to 26% of mean aerodynamic $\bar{C}$.

It is worth noting that the center of pressure keeps varying with angle of attack. Why? Because C_L keep varying here from this equation **.**At the same time, you know as angle of attack changes, the pressure distribution changes. Once you have different pressure distribution, you have different centroid for that distribution. So x_{cp} keep varying whereas x_{ac} remains constant over a range of velocities whereas angle of attack always remains constant.

Till now we are talking about airfoils. Let us say if I extrude the airfoil, what you get is wing. The airfoil is also known as infinite wing or two-dimensional wing. The wing is a 3D object whereas airfoil is a 2D object and is termed as infinite wing. Now since the wing is a 3D object it is worth talking about its planform geometry.

Wing Geometry and Planform Analysis

Here, let us talk about Wing Geometry.

For an aircraft, the wing and horizontal stabilizer are fundamental components influencing aerodynamic performance and stability. Typically, it is assumed that the wing extends up to the centerline of the aircraft, which corresponds to the fuselage reference line.

When measuring the planform geometry of a wing — which refers to the top view of the wing — the key geometric parameters include the span, root chord, and tip chord.

1. Span
The span is the lateral length of the wing, measured from one wingtip to the other. It represents the distance across the aircraft's wings in the lateral direction. The span is a critical parameter as it affects the lift generation and overall stability of the aircraft.

2. Chord
The longitudinal length of the wing, measured at any cross-section, is referred to as the chord. The chord represents the distance between the leading edge and the trailing edge of the wing at that specific cross-section.

- **Root Chord (c_root):** The chord length at the point where the wing meets the fuselage.
- **Tip Chord (c_tip):** The chord length at the wingtip.

These parameters define the planform shape of the wing and influence aerodynamic properties such as lift distribution, drag characteristics, and overall aerodynamic efficiency.

Let us consider

C_t = tip chord
C_R = root chord
S = area of the wing

B = span

Now let us talk about some of the non-dimensional parameters here of the wing. We define something called Aspect Ratio (AR)

$$AR = \frac{b^2}{S}$$

[3]There is no dimension for this. And for a delta wing configuration, the aspect ratio will be usually < 3 to < 5. We call them as Low Aspect Ratio wings. For a sail plain the aspect ratio will be from 8 to 16 and for glider it will be beyond 16.

Now let us define another parameter called Taper ratio (λ)

What are we tapering? We are tapering the chord. When you are reducing the chord length, we witness that the maximum thickness and everything will reduce. Hence, you are scaling down. When you say taper you are trying to reduce the chord length as we move along the span of the wing. So, the Taper ratio (λ)

$$\lambda = \frac{C_t}{C_R}$$

When we mention Taper ratio, are we missing anything? Do we require any additional information? Or when we talk about Taper is this λ sufficient enough or do we require any other information?

Let us consider the pointer whose radius is conical and the diameter is large compare to that of tip. For a cone, you have a bigger base and a smaller tip. The diameter has been reduced but the reduction has happened about a particular axis. For this particular pointer it happened about the longitudinal axis.

But for a wing what are the possibilities? If you look at the wing what you can see is it is tapered about trailing edge. That means your trailing edge of each and every airfoil are in the same location or in the same straight line. So, the wing is tapered above trailing edge. You require an axis about which you are tapering a wing i.e., axis for taper.

Let us consider a classical or a rectangular wing. What do you mean by rectangular wing? For a rectangular wing, at each and every point, you have equal chord. Let the chord be C. What will be the aspect ratio of a rectangular wing? For a rectangular wing, Aspect ratio is

$$AR = \frac{b^2}{S} = \frac{b^2}{b \times C} = \frac{b}{C}$$

Hence, the aspect ratio is (b/c).

Hence we will calculate the taper ratio.

$$\lambda = \frac{C_t}{C_R} = 1$$

Delta Wings and Sweep Angle

Let us now consider a triangular or delta wing configuration. In such a case, the tip chord (Ct) holds specific geometric significance. For a delta wing, the taper ratio (λ\lambda) is defined as:

$$\lambda = \frac{C_t}{C_R}$$

where:

- c_R Root chord (chord at the fuselage)
- c_T Tip chord (chord at the wingtip)

For a delta wing, the taper ratio is typically λ\lambda = 0 since the tip chord c_T is zero. The taper ratio, therefore, varies between 0 and 1 depending on the wing geometry.

Effect of Sweep Angle

Consider an initially rectangular wing. If the wing is rotated about a reference point, the wing takes on a swept configuration. This angular rotation introduces the concept of the **sweep angle** (denoted as λ\Lambda).

- When the wing is rotated backward, it creates a **sweepback angle** (λ\Lambda).
- Sweeping about the leading edge results in a **leading edge sweep**.
- Sweeping about the trailing edge gives a **trailing edge sweep**.
- Sweeping about the quarter chord results in a **quarter chord sweep**.

Impact on Aerodynamics

$$V_\infty \cos \Lambda$$

[7]When a wing is swept, the effective airflow seen by the airfoil changes. If the free-stream velocity is V_∞ component of velocity along the chord becomes:

This reduction in the effective velocity helps to delay the onset of compressibility effects and the critical Mach number on the airfoil. Although the aircraft may be flying at a certain Mach number with respect to the ground, the airfoil experiences a reduced Mach number due to the swept configuration.

Sweeping is especially beneficial at high speeds as it improves the critical Mach number and reduces wave drag. Additionally, both rectangular and tapered wings can be swept, combining the aerodynamic advantages of tapering and sweep for better high-speed performance.

Dihedral and Wing Geometry

Dihedral Angle

The dihedral angle refers to the angle formed between the wings and the horizontal plane when viewed from the front of the aircraft.

- If the wings are tilted upward from the wing root, the aircraft is said to have **positive dihedral**.
- If the wings are tilted downward, it is called **anhedral** or **negative dihedral**.

The dihedral angle plays a key role in providing **roll stability** to the aircraft.

- **Positive dihedral** increases lateral stability by creating a stabilizing rolling moment when the aircraft experiences sideslip.
- **Anhedral** is often used in high-performance jets and fighter aircraft to increase manoeuvrability at the cost of stability.

Importance of Sweep and Dihedral

- Sweep improves high-speed performance by delaying the onset of shock waves and compressibility effects.
- Dihedral enhances roll stability, particularly in general aviation and commercial aircraft.

Twist in Wings

Wing twist is the variation of the angle of incidence of the airfoil along the span of the wing. This can be of two types:

1. **Geometric Twist**
    - In geometric twist, the airfoil's angle of incidence changes along the span.
    - This is achieved by physically rotating the airfoil section along the span of the wing.
    - Geometric twist helps optimize the lift distribution and stall characteristics.
2. **Aerodynamic Twist**
    - In aerodynamic twist, the airfoil shape changes along the span without changing the physical angle of incidence.
    - This is done by using different airfoil sections along the span with varying camber and thickness.
    - Aerodynamic twist improves lift distribution and controls the stall pattern across the wing.

Wing Structure

Structurally, a wing is composed of several key components:

- **Ribs** – These provide the cross-sectional shape of the wing and define the airfoil.
- **Spars** – These are the main load-bearing elements that run along the span of the wing.
- **Skin** – The outer covering that provides the aerodynamic surface and contributes to the structural integrity.

Instead of using a solid wing, most aircraft wings are hollow to reduce weight while maintaining structural strength. The combination of ribs and spars creates a lightweight yet strong framework that is then covered with skin to create a smooth aerodynamic surface.

Wing Design for UAV Development

Wing Configuration and Structure

[8] For the UAV under development, the wing has a **2-meter span**, which is a scaled-down version of a larger wing with a full-scale span of **16 meters**. The wing is part of a **twin boom UAV** configuration, where the horizontal tail will be supported by two booms extending from the wing.

Key structural components include:

- **Ribs** – Positioned at regular intervals along the span to maintain the wing's aerodynamic shape and structural integrity.
- **Spars** – Main load-bearing elements running along the span of the wing to support aerodynamic and structural loads.
- **Carbon Fiber Tubes** – Reinforce the wing structure to provide strength and reduce weight.
- **Skin** – Covers the wing to provide a smooth aerodynamic surface and protect internal components.

The wing is **tapered**, with the chord length and thickness decreasing from the root to the tip. This taper improves aerodynamic efficiency and reduces induced drag.

Mean Aerodynamic Chord (MAC)

For a tapered wing, the chord length varies along the span. When analyzing aerodynamic forces and moments, a single reference length known as the **Mean Aerodynamic Chord (MAC)** is used to simplify calculations.

Definition of MAC:

$$\bar{c} = \frac{2}{S}\int_0^{b/2} c^2(y)\,dy$$

The Mean Aerodynamic Chord is defined as the chord length at which the aerodynamic center of the wing produces the same pitching moment as the entire wing.

where:

- Cbar = Mean Aerodynamic Chord
- S = Total wing area
- c(y) = Chord length at a distance yy along the span
- b = Wing span

The MAC allows the entire wing to be represented as a single airfoil with known lift, drag, and moment characteristics, simplifying aerodynamic analysis.

Aerodynamic Center

[9]The **Aerodynamic Center (AC)** is the point on the wing where the pitching moment remains constant with changes in the angle of attack. For symmetric airfoils, the aerodynamic center is typically located at the **quarter-chord point** (25% of the chord length).

For a tapered wing, the aerodynamic center is located at the quarter-chord point of the Mean Aerodynamic Chord. Knowing the position of the aerodynamic center is essential for calculating stability and control characteristics of the UAV.

Application to UAV

For the twin boom UAV:

- The MAC and aerodynamic center simplify the analysis of lift, drag, and pitching moment.
- Tapering the wing reduces induced drag and improves overall aerodynamic efficiency.
- The twin boom configuration enhances stability and control authority, particularly for high aspect ratio wings.

The general units are meters here. You have a root chord and you have a tip chord. Let us say the mean aerodynamic chord, $\bar{C}$ is given by

$$\bar{C} = \frac{2}{3} C_R \left(\frac{1 + \lambda + \lambda^2}{1 + \lambda} \right)$$

$$\lambda = \frac{C_t}{C_R}$$

Once you evaluate the above expression, you will end up getting a mean aerodynamic chord on either side which is symmetric. In case of a fixed string aircraft, the mean aerodynamic chord is projected onto the root chord or the fuselage reference line or the center line. And we witness that, the aerodynamic center lies at the 25% of the mean aerodynamic chord, $\bar{C}$.

Now, for a rectangular wing, let us say

$$\lambda = 1$$

From the equation of mean aerodynamic chord

$$\bar{C} = \frac{2}{3} C_R \left(\frac{3}{2} \right) = C_R$$

Hence, for a rectangular wing,

$$\bar{C} = C_R = C_t$$

What is the span wise distance (y_{mac}) at which the $\bar{C}$ is located? The span wise location of aerodynamic chord is

$$y_{mac} = \frac{b}{6} \left(\frac{1 + 2\lambda}{1 + \lambda} \right)$$

How to find aerodynamic center of wing.

It is 25% of MAC (Mean Aerodynamic Chord) measured from leading edge of $\bar{C}$.

Example: Find the aerodynamic center of the following UAVs.

Q1. Consider a pure delta wing. Let the be span be 2 meters and root chord be 1 meter. How to find the mean aerodynamic chord?

Solution:

Mean Aerodynamic Chord, $\bar{C}$ is given by

$$\bar{C} = \frac{2}{3} C_R \left(\frac{1 + \lambda + \lambda^2}{1 + \lambda} \right)$$

Given, $C_R = 1$ m

For a delta wing,

$$\lambda = \frac{C_t}{C_R} = \frac{0}{1} = 0$$

$$\bar{C} = \frac{2}{3} \times 1 \times 1 = \frac{2}{3} = 0.67m$$

Hence, the mean aerodynamic chord is 0.67 meters.

What exactly a delta wing is for? It is for a low speed. Assuming that there is no actual sweep here, the wing is tapered above trailing edge.

If there is a sweep you will take a component of this. That is, you will project the airfoil along the flow and you will take that airfoil as a rib to construct your wing.

But in this case, the low speed flows that we are talking are not going to give any sweep. In most of the cases, we consider the delta wing tapered above the trailing edge. Since it is tapered above trailing edge we can project directly because the trailing edge remains the same.

Aerodynamic center (AC) is 25% of the $\bar{C}$

$$AC = \frac{1}{4} \bar{C} = \frac{0.67}{4} = 0.167m$$

Hence, the aerodynamic center with respect to the leading edge is located at a distance of 0.167 meters.

What is the distance, $X_{ac,}$ from aerodynamic center?

$$x_{ac} = (C_R - \bar{C}) + 0 \cdot 25\bar{C}$$

$$x_{ac} = 33 \cdot 33 + 16 = 49 \cdot 7cm$$

49.7 cm which is approximately 0.5 meters. So the aerodynamic center lies at a distance of 0.5 meters from the nose of the delta wing.

APPENDIX-A: FRONT COVER AND EDGE

Aerodynamic Design and Optimization of a Fixed-Wing VTOL UAV with FDM-Based Manufacturing

2024

Aerodynamic Design and Optimization of a Fixed-Wing VTOL UAV with FDM-Based Manufacturing

SUBMITTED BY

Akash Pandey (Roll No. 11)

Avinash Mishra (Roll No. 16)

Sumit Paul (Roll No. 09)

Thesis submitted for the fulfillment of

the requirements for the degree

of

BACHELOR/MASTER OF TECHNOLOGY

Bachelor of Technology (B.Tech.)

Mechanical Engineering

INSTITUTE OF ENGINEERING & MANAGEMENT

MAULANA ABUL KALAM AZAD UNIVERSITY OF TECHNOLOGY,

WEST BENGAL

2024

REFERENCES

The examples of the referrals are given below:

Research journal articles:

[1]Raymer, D. P. (2012). *Aircraft design: A conceptual approach* (5th ed.). American Institute of Aeronautics and Astronautics.

[2]Anderson, J. D. (2017). *Fundamentals of aerodynamics* (6th ed.). McGraw-Hill Education.

[3]Gudmundsson, S. (2014). *General aviation aircraft design: Applied methods and procedures.* Butterworth-Heinemann.

[4]Brandt, S. A., Stiles, R. T., Bertin, J. J., & Whitford, R. (2004). *Introduction to aeronautics: A design perspective* (2nd ed.). American Institute of Aeronautics and Astronautics.

[5]Maughmer, M. D. (2003). Design optimization of winglets to maximize the performance of fixed-wing aircraft. *Journal of Aircraft, 40*(6), 1097–1100. https://doi.org/10.2514/2.718

[6]Chee Kai Chua, Kah Fai Leong, and Chu Sing Lim. Rapid Prototyping: Principles And Applications2nd Edition (with Companion CD-ROM), volume 1. World Scientific Publishing Co Inc, 2003. 3, 12, 16, 19

[7] Yunus Govdeli, Anh Tuan Tran, and Erdal Kayacan. Multiple Modeling and Fuzzy Switching Control of Fixed-Wing VTOL Tilt-Rotor UAV. In Fuzzy Tech niques: Theory and Applications, pages 270–284, Cham, 2019. Springer International

[8] Y. Govdeli, S. Muzaffar, R. Raunak, B. Elhadidi, and E. Kayacan. Unsteady Aerodynamic Modeling and Control of Pusher and Tilt-Rotor Quadplane Configurations.

[9] Joseph Katz and Allen Plotkin. Low-Speed Aerodynamics. Cambridge Aerospace Series. Cambridge University Press, 2 edition, 2001. doi: 10.1017/ CBO9780511810329. 4, 22, 7

Gmail

iem power

Compose

Inbox 6,431

Starred

Snoozed

Sent

Drafts 32

More

Labels

Congratulations! Your Abstract has been Accepted – IEMPOWER2025: Interr

Inbox ×

ScholarSpace <info@scholarspace.net>

to me

Dear Akash Pandey,

We are pleased to inform you that your abstract, **"Aerodynamic Design and Optimization of a Fixed-Wing VTOL UAV with FDM Mechanical Power**. Congratulations!

Abstract Details:

- **Abstract ID:** 54
- **Topic:** Track 3: Mechanical System Design & Optimization
- **Submitter Name:** Akash Pandey

Reviewer Comments:

1). Comment1: Your abstract is accepted

As the next step, you are invited to submit your **full manuscript** for further review. Please ensure that your submission follows the

You can log in to your dashboard to proceed: https://scholarspace.net.

If you have any questions or need assistance, feel free to reach out.

We look forward to your full manuscript submission and your participation in IEMPOWER2025: International Conference on Industr

Best regards,
ScholarSpace Team

One attachment • Scanned by Gmail

Aerodynamic Des